

Reduction of quantum noise in transmittance estimation using photon-correlated beams

Majeed M. Hayat

Electro-Optics Program, University of Dayton, Dayton, Ohio 45469-0245

Adel Joobeur

SVGL, 77 Danbury Road, MS 450, Wilton, Connecticut 06897-0877

Bahaa E. A. Saleh

Department of Electrical and Computer Engineering, Boston University, Boston, Massachusetts 02215-2421

Received May 26, 1998; revised manuscript received September 21, 1998; accepted September 25, 1998

The accuracy of optical measurements at low light levels is limited by the quantum noise of the source and by the random nature of the interaction with the measured object. The source noise may be reduced by use of nonclassical photon-number squeezed light. We consider the use of two photon-correlated beams (generated, for example, by spontaneous parametric downconversion) to measure the optical transmittance of an object. The photons of each beam obey a random Poisson process but are synchronized in time. One beam is used to probe the object, and the other is used as a reference providing information on the realization of the random arrival of photons at the object. The additional information available by such measurement may be exploited to improve the accuracy of the measurement. Various estimators, including the maximum-likelihood estimator, are considered, and their performance is evaluated and compared with the measurement based on a single-beam conventional (Poissonian) source and a maximally squeezed (fixed-photon-number) source. The performance advantage that is established depends on parameters such as the intensity of the source, the transmittance of the object, the quantum efficiency of the detectors, the background noise, and the degree of correlation of the photon numbers in the two beams. © 1999 Optical Society of America [S0740-3232(99)00702-4]

OCIS codes: 270.6570, 030.5290, 030.4280, 030.5260, 030.6600.

1. INTRODUCTION

The accuracy of optical measurements is ultimately limited by the quantum nature of light, which dominates at low light levels when the number of photons per spatial and temporal resolution elements is small.¹⁻⁴ The uncertainty of the measurement is caused by the random fluctuations of the probing optical beam and the random nature of the process of interaction with the probed object. Consider, for example, the simple process of measuring the transmittance of an object by using coherent light as a probe. If we think of each photon of the probe as a particle that is transmitted through the object with a probability equal to the transmittance, then the estimation of the transmittance is akin to estimating the probability of success in a repeated random Bernoulli experiment. However, since the photons themselves arrive at the object at random, in accordance with a Poisson process, an additional uncertainty is introduced. For example, if no photon is received, this could indicate that the photon failed to be transmitted (was absorbed by the object, for example) or that it did not arrive at the object in the first place. In this simple scenario, there are two uncertainties: one associated with the random arrival of the photons at the target and another resulting from the nature of the transmission process—a process of random deletion

of photons. Efforts at reducing the noise in the probe beam have fueled an interest in generating amplitude-squeezed (sub-Poissonian) and quadrature-squeezed light, which are forms of nonclassical light.⁵⁻⁸

Another source of nonclassical light that has generated considerable interest in recent years is photon-correlated beams. Here the light source takes the form of two beams, the photons of each arrive in accordance with a random Poisson process, but the photons of the two beams are, under ideal conditions, perfectly synchronized in time and space. Photon-correlated beams can be generated, for example, by spontaneous parametric downconversion.⁹⁻¹³ This is a nonlinear process in which each of the photons of a pump interacts with a medium exhibiting the second-order nonlinear effect and creates a pair of photons, a twin, called the signal and the idler. Conservation of momentum ensures that if one photon is observed in one direction, its twin must be present in one and only one matching direction. If the pump is in a coherent state, the statistics of the photons in each of the twin beams obeys a Poisson process, but the two processes are, under ideal conditions, completely correlated. Since the joint statistics of the photons of this light source have reduced uncertainty, this light source is squeezed. Photon-correlated beams have been proposed for use in a

number of applications including optical communications, cryptography, and tests of the quantum theory of light.^{14–19}

Photon-correlated beams may be effectively used for optical measurements; for example, measurement of the transmittance (or the reflectance) of an object. One beam, say the signal, serving as a probe, is transmitting through the object, and both the transmitted signal beam and the idler beam are observed. The information obtained by observing the idler photons provides us with a copy of the realization of the twin signal beam before its transmission through the object. Such information may be used to improve the accuracy of the measurement. Early work on this problem includes a calculation of the improvement in the accuracy of estimation using an approximation based on the assumption that the mean number of photons collected is large.²⁰ This assumption is not applicable in situations when the illumination is weak. Since the need to enhance the accuracy of measurement beyond the conventional quantum-limited level often arises when the light is weak, there is need to develop a more general theory that establishes the conditions required for achieving an improvement in the estimation accuracy for various estimators of the transmittance, including realistic nonideal conditions such as the finite quantum efficiency of the detectors, the background noise, and the partially correlated nature of the twin beams. This is the purpose of the present paper. Although the paper is cast as a theory of estimation of the transmittance (or the reflectance) of an object, the results are also applicable to the measurement of quantum efficiency of a detector and to other radiometric measurements.

This paper is organized as follows. In Section 2 we develop benchmarks for assessing the performance of all the estimates of the transmittance. The mean square errors associated with the maximum-likelihood (ML) estimators are determined for a conventional single-beam setup using a conventional probe with Poisson-distributed photons and an ideal probe with a deterministic number of photons arriving at the detector in a given time interval. These errors represent the standard single-beam quantum-limited performance and the random-deletion-limited performance, respectively. In Section 3 we consider three estimators based on measurements with photon-correlated beams and determine their associated errors. In Section 4 we examine the effect of various parameters on the performance improvement offered by the photon-correlated-beams measurement relative to that from the classical single-beam measurement. These parameters include the mean photon flux of the probe beam(s), the level of the transmittance to be estimated, the quantum efficiencies of the detectors used in the measurement, the level of background noise, and the degree of correlation between the photons of the twin beams.

2. SINGLE-BEAM MEASUREMENT

Consider the measurement of the transmittance t of a partially transmitting object by a conventional single-beam setup, as illustrated in Fig. 1. The probe beam carries an average photon flux λ (photons per second), which

is reduced to an average photon flux of $t\lambda$ upon transmission through the object. The transmitted beam is detected by using a detector with quantum efficiency η operated in the photon-counting mode and subjected to background noise equivalent to an average rate of μ photons per second. Such noise results from stray light and free charges that are thermally generated in the detector. The photon counter measures the number of counts N detected in a time duration T . This number is a random variable with mean value $\eta t\lambda T + \eta\mu T$.

The estimation problem at hand is as follows: Given the measured random variable N , and assuming that the parameters λ , μ , and η are known (from prior accurate measurements of the probe beam and the detector), find an estimate \hat{t} of the transmittance t . This estimate is of course a function of the measurement N , and this dependence will be explicitly denoted by $\hat{t}(N)$ whenever necessary. We also assume knowledge of a probabilistic model for the overall system, which is used to determine the probability distribution $P_N(k) = P(N = k)$ of the random variable N , where P stands for probability of an event. A common measure of performance of the estimator is the mean square error, defined by

$$\epsilon^2 = E[(\hat{t} - t)^2] = \sum_{k=0}^{\infty} [\hat{t}(k) - t]^2 P_N(k). \quad (1)$$

This error is of course dependent on the chosen estimator \hat{t} and on the probability distribution $P_N(k)$.

The simplest estimator is based on equating the measured random variable N with its expected value, i.e., $N = \eta t\lambda T + \eta\mu T$, or $\hat{t} = (N - \eta\mu T)/\eta\lambda T$. This estimator is generally not an optimal estimator, and it does not make use of the knowledge of the probability distribution of the measurement N . We shall consider instead the ML estimator. For a given detected count $N = k$, the ML estimator \hat{t}_{ML} is the value of t that maximizes the probability distribution function of the detected count N evaluated at k . ML estimators are widely used in signal detection and estimation.²¹

To determine the probability distribution $P_N(k)$, we consider the physical model in Fig. 1. Let N_s represent the random number of photons in the probe beam in the counting time T . Upon transmission through the object and detection by the detector, these photons generate a random number of counts N_{ds} in the counter. If N_n is

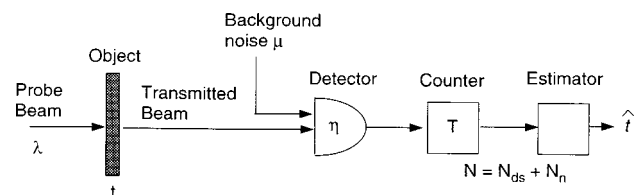


Fig. 1. Schematic diagram of single-beam measurement. A probe beam with photon flux λ is transmitted through an object with transmittance t , and the photon count N (in an interval T) is measured by using a detector (with quantum efficiency η) and a counter. The background-noise photon flux is μ . The measurement N is the sum of the detected probe beam photons N_{ds} and the detected background photons N_n . A single-beam estimator uses the photon count N to generate an estimate \hat{t} of t .

the random number of background counts, then $N = N_{ds} + N_n$. The random number N_{ds} is a deleted version of the random number N_s , where every count of N_s survives with probability ηt . The expected values of these random variables are $E(N_s) = \lambda T$, $E(N_{ds}) = \eta t \lambda T$, and $E(N_n) = \eta \mu T$. To determine the probability distribution of N , we need to specify the statistics of N_s and N_n . We shall consider two special cases for the statistics of the probe beam photocounts N_s .

1. N_s is a fixed deterministic number (corresponding to maximum photon-number squeezing), and

2. N_s has a Poisson distribution (corresponding to coherent or classical light). In this case $P_{N_s}(k) = P(\eta \lambda; k)$, where $P(\delta; k) = \exp(-\delta) \delta^k / k!$ is the Poisson probability distribution function with mean δ .

As for the statistics of the background counts N_n , we shall assume that it obeys the Poisson statistics, i.e., $P_{N_n}(k) = P(\eta \mu T; k)$. Our experience, however, indicates that the exact statistics of the background noise is not critical to cases of interest to us here when the mean value of the background count is low.

A. Probe Beam with Fixed Number of Photons

In ideal antibunched light,⁶ the photon stream is maximally regularized, and the number of photons arriving at the detector in any time interval is deterministic. This situation corresponds to light in a maximally photon-number squeezed state. In this case the probability distribution function of the number of photons arriving at the detector in T units of time in the probe beam is given by

$$P_{N_s}(k) = \delta(k - n), \quad (2)$$

where $\delta(k) = 1$ if $k = 0$ and $\delta(k) = 0$ otherwise. In general, the Mandel parameter,²² which is a measure of uncertainty in the photon count, is defined as

$$Q(0) = \frac{E[(N_s - \bar{N}_s)^2]}{\bar{N}_s} - 1, \quad (3)$$

(where \bar{N}_s is the mean of N_s), and it assumes a minimum value of -1 in the case of maximally photon-number squeezed light. Clearly, uncertainty in transmittance estimation with a direct detection scheme will be at its minimum for this maximally photon-number squeezed state. Each photon is transmitted through the object with probability t . The combined effect of the transmission and detection process on the probe beam photons can be thought of as a random-deletion process for which the probability that a photon is transmitted and detected is ηt . Thus the number of detected photons N_{ds} is a binomial random variable (a sum of n independent binary random variables) whose probability distribution function is given by

$$P_{N_{ds}}(k) = B(n, \eta t; k), \quad (4)$$

where

$$B(n, \eta t; k) = \binom{n}{k} (\eta t)^k (1 - \eta t)^{n-k} \quad (5)$$

is a binomial probability distribution function with parameters n and ηt . If we use the fact that N_{ds} and N_n are statistically independent, the probability distribution of the detected count N is given by the discrete convolution²³

$$P_N(k) = \sum_{i=0}^{\min(n, k)} B(n, \eta t, i) P(\eta \mu T; k - i). \quad (6)$$

The ML estimator $\hat{t}_{F,ML}$, for a given count observation k , is the value of t that maximizes Eq. (6). It can be shown that this maximizer is the solution, in the interval $[0,1]$, of the following equation:

$$\frac{d}{dt} P_N(k) = \sum_{i=0}^{\min(n, k)} \left[\frac{i}{t} - \frac{\eta(n-i)}{1-\eta t} \right] \times B(n, t \eta, i) P(\eta \mu T; k - i) = 0. \quad (7)$$

If such a solution does not exist, then $\hat{t}_{F,ML}$ is set to the appropriate end point (zero or one). In Section 4 the above equation is solved numerically to obtain $\hat{t}_{F,ML}$.

The mean square error in the transmittance estimation, $\epsilon_{F,ML}^2$, is evaluated by using Eqs. (1) and (6) and the numerically computed ML estimator $\hat{t}_{F,ML}$ given by Eq. (7). This error represents the random-deletion-limited performance in the single-beam case. This error is used hereafter as a benchmark for comparison with results based on photon-correlated beams.

B. Probe Beam with Poissonian Photon Number

In the case of a probe beam with Poissonian photon statistics, the probability distribution function of the number of detected photons N_{ds} is Poissonian with rate $\eta t \lambda$. Furthermore, since the overall count N is an independent sum of two Poisson random variables, it too is a Poisson random variable. The probability distribution function of N is therefore

$$P_N(k) = P(\eta t \lambda T + \eta \mu T; k). \quad (8)$$

[In this case the Mandel parameter $Q(0) = 0$.] If Eq. (8) is maximized over t , the ML estimator $\hat{t}_{P,ML}$ can be explicitly determined in terms of the number of observed counts N :

$$\hat{t}_{P,ML} = \begin{cases} 0 & \text{if } \frac{N}{\eta \lambda T} \leq \frac{\mu}{\lambda} \\ 1 & \text{if } \frac{N}{\eta \lambda T} \geq 1 + \frac{\mu}{\lambda} \\ \frac{N}{\eta \lambda T} - \frac{\mu}{\lambda} & \text{otherwise} \end{cases} \quad (9)$$

The hard limiting that appears in Eq. (9) plays a role only in situations when the photon count is low. The effect of this hard limiting may be neglected otherwise.

The mean square error $\epsilon_{P,ML}^2$ in this case can be numerically calculated by using Eqs. (1), (8), and (9). When the mean photon count $(\eta t \lambda + \eta \mu) T$ is sufficiently high to warrant neglecting the hard-limiting effect in the expression of $\hat{t}_{P,ML}$, the mean square error $\epsilon_{P,ML}^2$ takes the simple form

$$\epsilon_{P,ML}^2 = \frac{1}{\eta\lambda T} \left(t + \frac{\mu}{\lambda} \right). \quad (10)$$

In the ideal case when $\mu = 0$ and $\eta = 1$, $\epsilon_{P,ML}^2$ is the error that is due only to the combined effect of quantum noise and random deletion of photons. This error is due to noise associated with random deletion, represented by $\epsilon_{F,ML}^2$, and to noise associated with photon-number fluctuation. Since a Poissonian light is the limit in photon fluctuation noise in the semiclassical theory, $\epsilon_{P,ML}^2$ represents the standard quantum limit of transmittance estimation noise. By using squeezed light sources, we can reduce the transmittance noise to almost $\epsilon_{F,ML}^2$, which is the lowest mean square error in transmittance estimation using direct detection.

3. MEASUREMENT WITH PHOTON-CORRELATED BEAMS

In this section we consider the problem of measuring the transmittance of an object by using two photon-correlated beams, one used as a probe (signal beam) and the other as a reference (idler beam). The estimation setup is shown schematically in Fig. 2.

The signal beam passes through the partially transmitting object, as in the case of the single-beam setup of Section 2. The second beam, the idler, does not go through the object and is used to provide information on the actual number of photons N_s in the signal beam. After transmission and detection (with detection quantum efficiency η_s), N_s is reduced to the detected number of signal photons N_{ds} . The total number of counts in the signal chan-

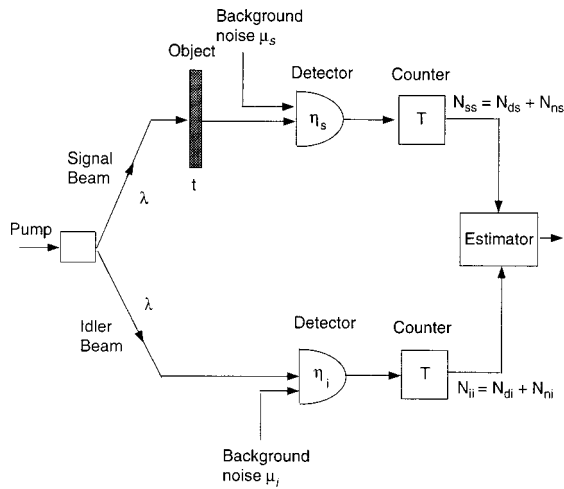


Fig. 2. Schematic diagram of measurement with photon-correlated beams. The signal beam (with photon flux λ) is used as a probe and transmitted through the object (with transmittance t), and the idler beam (also with photon flux λ) is used as a reference. The observed output N_{ss} of the signal-channel counter is the sum of the detected photons N_{ds} , in the duration T , resulting from the transmitted signal beam and the detected background photons N_{ns} . The observed output N_{ii} of the idler-channel counter is the sum of the detected photons N_{di} resulting from the idler beam and the detected background photons N_{ni} . The quantum efficiencies of the detectors in the signal and idler channels are η_s and η_i , respectively. A photon-correlated estimator uses the observations N_{ss} and N_{ii} to generate an estimate \hat{t} of t .

nel, N_{ss} , is the sum of N_{ds} and the additive background noise in the signal channel, denoted by N_{ns} . The number of photons from the idler beam, N_i , is in turn reduced after detection in a photon counter (with quantum efficiency η_i) to N_{di} . The total number of counts in the idler channel, N_{ii} , is the sum of N_{di} and the background noise in the idler channel, N_{ni} . A transmittance estimator \hat{t} in the photon-correlated light setup is a function of both N_{ss} and N_{ii} . As in Section 2, we assume that the additive independent background-noise photon counts N_{ns} and N_{ni} are Poissonian with means $\eta_s\mu_s T$ and $\eta_i\mu_i T$, respectively.

The statistics of the signal and idler counts are described by the joint probability distribution $P_{N_s N_i}(k, l) = P(N_s = k, N_i = l)$. Under ideal conditions the signal and idler photons are fully correlated, and $P_{N_s N_i}(k, l) = \delta(k - l)P_{N_s}(k)$, where $P_{N_s}(k) = P(N_s = k)$ is the probability distribution function of the number of signal photons. Such conditions are achieved in spontaneous parametric downconversion when the pump is a monochromatic plane wave, the crystal dimensions are infinite, and the signal and idler beams are selected by perfectly matched apertures. In practice, these conditions are not met, and the collected signal and idler beam photons are not fully correlated even when matched apertures are used.^{12,13} Additionally, the transmission of the signal and idler beams through optical elements results in further reduction of the degree of correlation.²⁴

To account for the partial correlation of the signal and idler photon numbers, we adopt a simplified model in which the counts are sums of totally correlated components and totally uncorrelated components: $N_s = N_t + N_{us}$ and $N_i = N_t + N_{ui}$, where N_t is a random number with mean $(1 - \beta)\lambda T$, representing the fully correlated component, and N_{us} and N_{ui} are statistically independent and identically distributed random variables with mean $\beta\lambda T$. This assumption is valid for matched apertures.¹³ The parameter β therefore represents the fraction of the uncorrelated photons in the signal and idler beams. The case $\beta = 0$ corresponds to full correlation. For simplicity we also use a Poisson model for these random variables, so that

$$P_{N_t}(k) = P((1 - \beta)\lambda T; k), \quad (11)$$

$$P_{N_{us}}(k) = P_{N_{ui}}(k) = P(\beta\lambda T; k). \quad (12)$$

We now determine the joint probability distribution function of the observed counts, $P_{N_{ss} N_{ii}}$. To simplify the derivation, we first note that the uncorrelated signal and idler photons N_{us} and N_{ui} can be combined with the additive background noise N_{ns} and N_{ni} , respectively. Thus the probability distribution functions of the independent random variables $N_{us} + N_{ns}$ and $N_{ui} + N_{ni}$ are $P(\eta_s t \beta \lambda + \eta_s \mu_s; k)$ and $P(\eta_i \beta \lambda + \eta_i \mu_i; k)$, respectively. Next we observe that, conditioned on the event that the number of twin photons $N_t = n$, the random counts N_{ss} and N_{ii} are independent, since the correlation between N_{ss} and N_{ii} is through N_t alone. Hence, by using this conditional independence and an argument similar to the one used in deriving Eq. (6), we can write an

expression for the conditional joint probability distribution function of N_{ss} and N_{ii} as the product

$$P_{N_{ss}N_{ii}|N_t}(k, l|n) = \sum_{i=0}^{\min(n, k)} B(n, t\eta_s; i)P(\beta\lambda t\eta_s T + \eta_s\mu_s T; k-i) \times \sum_{j=0}^{\min(n, l)} B(n, \eta_i; j)P(\beta\lambda\eta_i T + \eta_i\mu_i T; l-j). \quad (13)$$

The joint probability distribution function $P_{N_{ss}N_{ii}}(k, l)$ can now be obtained by averaging Eq. (13) over all possible values of N_t :

$$P_{N_{ss}N_{ii}}(k, l) = \sum_{n=0}^{\infty} P(\beta\lambda T; n) \left[\sum_{i=0}^{\min(n, k)} B(n, t\eta_s; i) \times P(\beta\lambda t\eta_s T + \eta_s\mu_s T; k-i) \sum_{j=0}^{\min(n, l)} B(n, \eta_i; j) \times P(\beta\lambda\eta_i T + \eta_i\mu_i T; l-j) \right]. \quad (14)$$

The mean square error ϵ_t^2 associated with any photon-correlated estimator \hat{t} can now be evaluated as follows:

$$\epsilon_t^2 = \sum_{k=0}^{\infty} \sum_{l=0}^{\infty} [\hat{t}(k, l) - t]^2 P_{N_{ss}N_{ii}}(k, l). \quad (15)$$

The estimators considered in this section rely on the positive correlation between the detected signal and idler photons to obtain an estimation error that is below the standard quantum limit error level. It is interesting to observe that although the probability distribution function of the total signal counts N_{ss} is Poissonian, the conditional distribution of N_{ss} given N_{ii} is sub-Poissonian as long as $\beta < 1$. This conditional distribution can be obtained by dividing the joint distribution in Eq. (14) by the Poissonian distribution of N_{ii} . To establish a quantitative connection between this conditional sub-Poissonian light and amplitude-squeezed light, we define the conditional Mandel Q factor (given that $N_t = n$) as

$$Q^c(n) = \frac{E[(N_{ss} - \bar{N}_{ss})^2 | N_t = n]}{\bar{N}_{ss}} - 1, \quad (16)$$

where \bar{N}_{ss} is the mean of N_{ss} . For the case $\mu_s = \mu_i = 0$ and ideal detection, it can be shown that

$$Q^c(n) = \frac{\beta\lambda T}{n + \beta\lambda T} - 1. \quad (17)$$

The average Mandel Q factor \bar{Q} can now be defined by averaging Eq. (17) over n . We have numerically evaluated the average Mandel parameter \bar{Q} , and the results show that $\bar{Q} = \beta - 1$, which is exactly the fraction of correlated photons in the beams. Hence, if $\beta = 0$, the average conditional Mandel parameter is equivalent to that of maximal amplitude squeezing. In contrast, when β

$= 1$, the average conditional Mandel parameter is equal to that of Poissonian light. Thus a photon-correlated pair of beams resembles a single amplitude-squeezed beam in the sense of reducing the uncertainty of the number of photons. This reduction in the average conditional Mandel parameter is manifested in the improved performance of transmittance estimation using photon-correlated beams. The connection between the Mandel parameter and noise in measurement in other applications has been considered in the literature. For example, the dependence of the photocurrent noise in short-pulse direct detection of nonclassical light has been investigated by Huttner *et al.*²⁵ The conditional variance reduction phenomenon has also been investigated in other applications.²⁶

We now develop three estimators and investigate their performance: the ML estimator, the count-ratio estimator, and the count-difference estimator.

A. Maximum-Likelihood Estimator

For given observed signal-channel and idler-channel photon counts $N_{ss} = k$ and $N_{ii} = l$, respectively, the ML estimator $\hat{t}_{C,ML}(k, l)$ is obtained by maximizing the joint probability distribution function $P_{N_{ss}N_{ii}}(k, l)$ given in Eq. (14). The maximization can be achieved by setting the derivative (with respect to t) of $P_{N_{ss}N_{ii}}(k, l)$ to zero and solving for t . The resulting equation is

$$\sum_{n=0}^{\infty} P(\lambda T; n) \left\{ \sum_{i=0}^{\min(n, k)} \left[\frac{i}{t} - \frac{\eta_s(n-i)}{1-t\eta_s} - \beta\lambda\eta_s T + \frac{\beta\lambda\eta_s T(k-i)}{\mu_s\eta_s T + \beta\lambda t\mu_s T} \right] \times B(n, t\eta; i)P(\beta\lambda t\eta T + \eta\mu T; k-i) \times \sum_{j=0}^{\min(n, l)} B(n, \eta; j)P(\beta\lambda\eta T + \eta\mu T; l-j) \right\} = 0. \quad (18)$$

Equation (18) is solved numerically to obtain $\hat{t}_{C,ML}(k, l)$. When the solution to Eq. (18) is not in the interval $[0, 1]$, the estimate $\hat{t}_{C,ML}$ is appropriately set to either 0 or 1. Using this expression of the transmittance estimate and the expression of the joint probability of the detected counts in Eq. (14), we can evaluate the estimation mean square error. The results and the discussion are deferred to Section 4.

B. Count-Ratio Estimator

This estimator is based on the ratio of counts N_{ss}/N_{ii} , which was first proposed by Jakeman and Rarity.²⁰ The motivation for developing this estimator is the fact that the ratio of the means of N_{ss} and N_{ii} is proportional to $t + \mu_s/\lambda$. The ratio N_{ss}/N_{ii} therefore contains information on the unknown parameter t . The procedure that we follow to get the general form of this estimator is to determine the mean $E(N_{ss}/N_{ii})$ and express t in terms of this mean. The ratio estimator $\hat{t}_{C,R}$ is obtained by replacing $E(N_{ss}/N_{ii})$ in the expression for t by the observed ratio N_{ss}/N_{ii} . We show in Appendix A that

$$\hat{t}_{C,R}(N_{ss}, N_{ii}) = \frac{1}{\alpha_R} \frac{N_{ss}}{N_{ii}} - \frac{\beta_R}{\alpha_R}, \quad (19)$$

where

$$\alpha_R = \eta_s \lambda T \left\{ \frac{1 - \exp[-\eta_i(\lambda + \mu_i)T]}{(\lambda + \mu_i)T} + (1 + \beta - \eta_i) \mathbf{E}[N_{ii}^{-1} u(N_{ii})] \right\}, \quad (20)$$

$$\beta_R = \eta_s \mu_s T \mathbf{E}[N_{ii}^{-1} u(N_{ii})], \quad (21)$$

and the function $u(\cdot)$ is the unit-step function [$u(x) = 1$ if $x > 0$ and $u(x) = 0$ otherwise]. The derivation of $\hat{t}_{C,R}$ is based on iterated conditional expectations and Bayes's theorem. The expectation $\mathbf{E}[N_{ii}^{-1} u(N_{ii})]$ is computed numerically in Section 4. Values of $\hat{t}_{C,R}$ that are in excess of unity or less than zero are hard limited to unity and zero, respectively. It turns out that, as in the case of the ML estimator $\hat{t}_{C,ML}$, the effect of hard limiting is negligible unless the photon counts are very small.

A careful examination of $\hat{t}_{C,R}$ reveals that in the special case when $\eta_i = 1$, $\beta = 0$, and $\mu_s = 0$, no hard limiting is required, and, further, that if $\mu_i = 0$, then $\hat{t}_{C,R}$ is in fact equivalent to the ML estimator $\hat{t}_{C,ML}$. However, the ML estimator does exhibit a performance advantage over the ratio estimator in general, as can be seen from the examples of Section 4. The mean square error $\epsilon_{C,R}^2$ associated with $\hat{t}_{C,R}$ can be evaluated numerically by using Eqs. (14) and (19) in Eq. (15). The results and a discussion are presented in Section 4.

The simplicity of the ratio estimator facilitates deriving an explicit upper bound for $\epsilon_{C,R}^2$. This upper bound is then used to determine the asymptotic behavior of $\epsilon_{C,R}^2$ in the limit when λ or T is large. In particular, an asymptotic analysis can be carried out to show that the behavior of $\epsilon_{C,R}^2$ for large values of the intensity λ (assuming that $\beta = 0$) is given by

$$t \{ \eta_s^{-1} - \eta_i t [1 - (1 - \eta_i^{-1})^2] \} \lambda^{-1} + o(\lambda^{-1}). \quad (22)$$

The above expression shows, as expected, that $\epsilon_{C,R}^2 \rightarrow 0$ as $\lambda \rightarrow \infty$. The asymptotic expansion in expression (22) is used in Section 4 to determine the asymptotic advantage of the count-ratio estimator $\hat{t}_{C,R}$ over the Poissonian single-beam estimator $\hat{t}_{P,ML}$.

C. Count-Difference Estimator

We now develop an estimator based on the difference between the photon counts N_{ss} and N_{ii} . The motivation is that in the ideal case of unit quantum efficiency, the difference $N_{ss} - N_{ii}$ represents the number of photons that are not transmitted through the object, and its mean is simply $(1 - t)\lambda$. More importantly, the average effect of background noise can be reduced, since N_{ns} and N_{ni} are subtracted from each other. As in the case of the ratio estimator, to derive the estimator $\hat{t}_{C,D}$, we first express $\mathbf{E}(N_{ss} - N_{ii})$ in terms of t and then solve for t . The calculations in this case are much simpler, and the resulting expression is

$$\hat{t}_{C,D}(N_{ss}, N_{ii}) = \frac{1}{\alpha_D} (N_{ss} - N_{ii}) - \frac{\beta_D}{\alpha_D}, \quad (23)$$

where

$$\alpha_D = \eta_s \lambda T, \quad (24)$$

$$\beta_D = \eta_s \mu_s T - \eta_i \mu_i T - \eta_i \lambda T. \quad (25)$$

This choice of the coefficients α_D and β_D makes the above estimator unbiased. However, once this estimate is hard limited to avoid situations when Eq. (23) is outside the range $[0, 1]$, some bias is introduced. This bias is negligible for reasonably large signal photon rates. The asymptotic behavior of $\epsilon_{C,D}^2$ for large values of λ can be shown to be

$$\epsilon_{C,D}^2 = \frac{1}{\eta_1 T} \left\{ t [1 - 2\eta_2(1 - \beta)] + \frac{\eta_2}{\eta_1} \right\} \lambda^{-1} + o(\lambda^{-1}), \quad (26)$$

which approaches zero at a rate of $1/\lambda$ as λ increases.

4. DISCUSSION OF RESULTS

We have so far considered three situations for the measurement of the transmittance of an object: conventional (Poisson) single-beam measurement, maximally squeezed (fixed-photon-number) single-beam measurement, and correlated twin-beam measurement. We have denoted these three cases by the symbols P, F, and C, respectively. We have also examined three types of estimator: ML estimator, count-ratio estimator, and count-difference estimator. We have denoted these by the symbols ML, R, and D, respectively. In this section we determine the error ϵ for these situations and estimators. As a relative measure of the performance of a given estimator with respect to the standard quantum-limited performance, we introduce the improvement factor ρ , for each estimator, as the ratio of the estimation error to the error associated with the Poissonian single-beam ML estimator $\hat{t}_{P,ML}$:

$$\rho = \frac{\epsilon}{\epsilon_{P,ML}}. \quad (27)$$

To evaluate ϵ and ρ for each estimator, the probability distributions (6) and (14) are computed numerically. To compute the photon-correlated-beams ML estimator $\hat{t}_{C,ML}$ and the ML estimator using a fixed number of photons, $\hat{t}_{F,ML}$, Eqs. (7) and (18) are solved numerically by using the joint probability distributions (6) and (14), respectively. To achieve high computational accuracy and speed and to avoid computer overflow, recursive algorithms (using C programming) were developed to carry out the above computations. For convenience we denote the mean number of signal photons per estimation time λT by n .

A. Asymptotic Performance Advantage

Before presenting the numerical results, we will examine the asymptotic behavior of the improvement factor ρ for the count-ratio estimator $\hat{t}_{C,R}$ and the count-difference estimator $\hat{t}_{C,D}$. Using Eq. (10) and expression (22), we obtain

$$\lim_{n \rightarrow \infty} \rho_{\hat{t}_{C,R}}^2 = 1 - \eta_s(2 - \eta_i^{-1})t. \quad (28)$$

Similarly, we can use Eqs. (10) and (26) to obtain

$$\lim_{n \rightarrow \infty} \rho_{\hat{t}_{C,D}}^2 = \frac{\eta_i}{\eta_s t} + [1 - 2\eta_i(1 - \beta)]. \quad (29)$$

From Eq. (28) we deduce that for any η_s , $t > 0$, and $\eta_i > 0.5$, there exists a threshold level n beyond which $\rho_{\hat{t}_{C,R}} < 1$. This implies that the count-ratio estimator $\hat{t}_{C,R}$ can outperform the Poissonian single-beam ML estimator as long as n and η_i are sufficiently high. Jakeman and Rarity²⁰ showed that in the absence of background-noise photons, a performance advantage is possible if both η_s and η_i are greater than 0.5. Our result therefore guarantees a performance advantage under weaker conditions. On the other hand, Eq. (29) indicates that the possible performance advantage associated with the count-difference estimator $\hat{t}_{C,D}$ is very sensitive to the transmittance t . In particular, and unlike the case for $\hat{t}_{C,R}$, even under ideal detection conditions ($\eta_s = \eta_i = 1$) and full photon correlation ($\beta = 0$), no performance advantage over the Poissonian single-beam estimator $\hat{t}_{P,ML}$ is predicted when t is very small.

B. Performance Advantage under Ideal Conditions

We now investigate the performance of the various estimators under the ideal conditions of unit quantum efficiencies, no background photons, and fully photon-correlated beams ($\beta = 0$). Figure 3(a) shows the error ϵ in the transmittance estimation as a function of the transmittance t , and Fig. 3(b) shows the dependence of the improvement factor ρ on t . As expected, the fixed-photon-number ML estimator $\hat{t}_{F,ML}$ incurs the smallest absolute estimation error ϵ . This error is the random-deletion-limited error, and it is the best possible performance in transmittance estimation. Confirming the theory presented in Subsection 3.B, the count-ratio and ML estimators are identical under these ideal conditions. The error associated with the fixed-photon-number ML estimator $\hat{t}_{F,ML}$, the photon-correlated-beams ML estimator $\hat{t}_{C,ML}$, and the count-ratio estimator $\hat{t}_{C,R}$ are symmetric about $t = 0.5$. This is due to the fact that the uncertainty in these estimators, under the given ideal conditions, is almost exclusively due to the process of photon random deletion [which typically exhibits a variance involving the symmetric term $t(1 - t)$]. Specifically, the quantum uncertainty is totally absent in the case of $\hat{t}_{F,ML}$, and it is brought to a minimum in the case of $\hat{t}_{C,ML}$ and $\hat{t}_{C,R}$ as a result of the additional information provided by the idler beam. In contrast, the behavior of the Poissonian single-beam ML estimator $\hat{t}_{P,ML}$ does not exhibit any symmetry in the transmittance t . This lack of symmetry is attributed to quantum noise, which is strongly signal dependent: the higher t is, the higher is the number of signal photons, which in turn results in a higher absolute variability in the signal photon. This effect results in an increase in the absolute error ϵ . The dip in the curve of $\epsilon_{\hat{t}_{P,ML}}$ near $t = 1$ is a clear indication of the hard-limiting operation involved in the single-beam estimator. The ef-

fect of the hard limiting for the single-beam ML estimator becomes noticeable for values of t near unity, since there is an increased likelihood of the number of detected photons N exceeding $\eta\lambda T$.

The asymmetric behavior (about $t = 0.5$) of the error associated with the count-difference estimator $\hat{t}_{C,D}$ can be explained in the context of the asymmetry seen in $\epsilon_{\hat{t}_{P,ML}}^2$ and by keeping in mind that the mean of $N_{ss} - N_{ii}$ is proportional to $1 - t$ rather than t . The absolute difference between the error associated with the ML fixed-photon-number estimator and that of any one of the other estimators represents the error that is due to the quantum fluctuation of the number of source signal photons. Clearly, with the exception of $\hat{t}_{C,D}$, all the photon-correlated-beams estimators exhibit a superior performance in comparison with that of the conventional single-beam ML estimator $\hat{t}_{P,ML}$ for all values of the parameter t [see Fig. 3(b)]. Furthermore, the improvement factor ρ decreases with t . As for the count-difference estimator, the improvement factor ρ is less than unity as long as $t > 0.5$. This behavior is predicted by the asymptotic expression (29). The improvement factor ρ is in general a strong function of n and is least for the fixed-photon-number estimator $\hat{t}_{F,ML}$, reaching a minimum value of -1.6 dB at $n = 4$ (see Fig. 4). The improvement factor for the photon-correlated-beams estimators $\hat{t}_{C,R}$ and $\hat{t}_{C,ML}$ are approximately -1 dB in the low-photon-count range ($n < 20$). Furthermore, the performance of $\hat{t}_{C,R}$ and $\hat{t}_{C,ML}$ becomes very comparable with the random-deletion limit as n increases beyond 20. As expected from the asymptotic expression (28), $\rho_{\hat{t}_{C,R}} \rightarrow \sqrt{0.5}$ (-1.5 dB) as $n \rightarrow \infty$. As for the count-difference estimator $\hat{t}_{C,D}$, it starts off with a superior performance to that of the Pois-

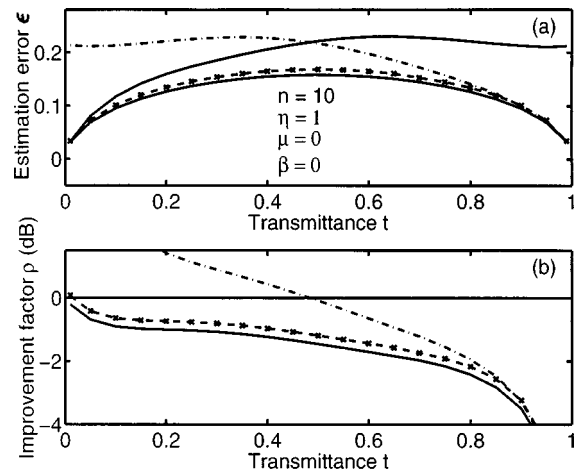


Fig. 3. (a) Estimation error ϵ as a function of the transmittance parameter t for the various estimators: Poissonian single-beam ML estimator $\hat{t}_{P,ML}$ (top solid curve), fixed-photon-number ML estimator $\hat{t}_{F,ML}$ (bottom solid curve), photon-correlated-beams ML estimator $\hat{t}_{C,ML}$ (dashed curve), count-ratio estimator $\hat{t}_{C,R}$ (represented by the symbol \times and overlaying the dashed curve), and count-difference estimator $\hat{t}_{C,D}$ (dotted-dashed curve). The estimation parameters are $n = 10$, $\eta_s = \eta_i = 1.0$, $\mu_s = \mu_i = 0$, and $\beta = 0$. Note the complete overlap between the count-ratio estimator curve and the photon-correlated-beams ML estimator curve. (b) Improvement factor ρ as a function of t . The curve symbols are same as in (a).

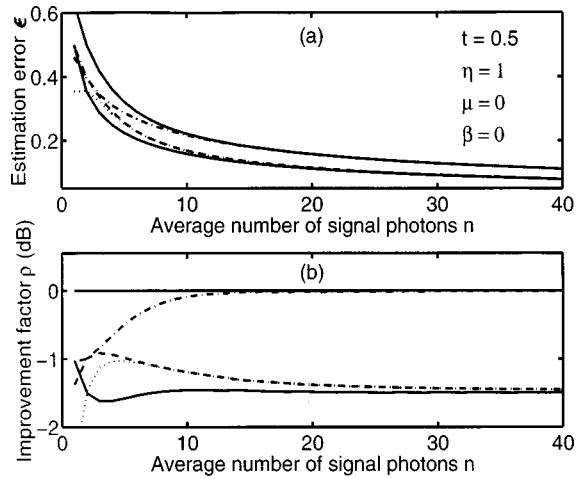


Fig. 4. (a) Estimation error ϵ as a function of the mean number of signal photons n for the various estimators: Poissonian single-beam ML estimator $\hat{t}_{P,ML}$ (top solid curve), fixed-photon-number ML estimator $\hat{t}_{F,ML}$ (bottom solid curve), photon-correlated-beams ML estimator $\hat{t}_{C,ML}$ (dashed curve just above the bottom solid curve), count-ratio estimator $\hat{t}_{C,R}$ (dotted curve just above the bottom solid curve), and count-difference estimator $\hat{t}_{C,D}$ (dotted-dashed curve). The estimation parameters are $t = 0.5$, $\eta_s = \eta_i = 1.0$, $\mu_s = \mu_i = 0$, and $\beta = 0$. Note the complete overlap between the count-ratio estimator curve and the photon-correlated-beams ML estimator curve. (b) Improvement factor ρ as a function of n .

sonian single-beam estimator $\hat{t}_{P,ML}$, but as n increases (approximately beyond 10), its performance approaches that of $\hat{t}_{C,ML}$. This result was also predicted from Eq. (29).

C. Effect of Nonideal Detectors and Background Noise

In general, the improvement associated with the correlated-photon-beams estimators ($\hat{t}_{C,D}$, $\hat{t}_{C,ML}$, and $\hat{t}_{C,R}$) and the fixed-photon-number estimator $\hat{t}_{F,ML}$ is reduced as a result of the presence of background noise and low quantum efficiency. Figure 5 shows the dependence of the error ϵ and the improvement factor ρ on the transmittance t for each estimator for the case $n = 20$, $\eta_s = \eta_i = 0.7$, $\mu_s = \mu_i = 5$, and $\beta = 0$. The results indicate that among all the photon-correlated-beams estimators, the ML estimator $\hat{t}_{C,ML}$ has the best performance (as expected). The improvement factor associated with $\hat{t}_{C,ML}$ is as low as -1.5 dB for a transmittance parameter $t = 0.9$. Nonetheless, for low values of the transmittance parameter t (e.g., $t < 0.3$), $\hat{t}_{C,ML}$ shows no improvement over the conventional ML estimator $\hat{t}_{P,ML}$ at such a low signal level n . The fact that $\hat{t}_{C,ML}$ results in a greater error than that from the conventional single-beam ML estimator $\hat{t}_{P,ML}$ seems counterintuitive at first, since one might suspect that $\hat{t}_{C,ML}$ should always be a better estimator than $\hat{t}_{P,ML}$, given that they are based on the same ML principle and the former enjoys the added benefit of the information contained in the idler-channel photons N_{ii} . However, one needs to keep in mind that a ML estimator does not necessarily generate a least mean square error.²¹ The performance of the count-ratio estimator $\hat{t}_{C,R}$ is slightly inferior to that associated with the photon-

correlated-beams ML estimator $\hat{t}_{C,ML}$, and the performance of the count-difference estimator $\hat{t}_{C,D}$ is the worst among all estimators (see Fig. 6). No improvement is obtained with the count-difference estimator for any value of n in this case. The improvement factor decreases with n for all the photon-correlated-beams estimators. As n increases beyond, approximately, 40, the improvement factor associated with $\hat{t}_{C,R}$ levels off at -0.84 dB, which is in agreement with the limit (28).

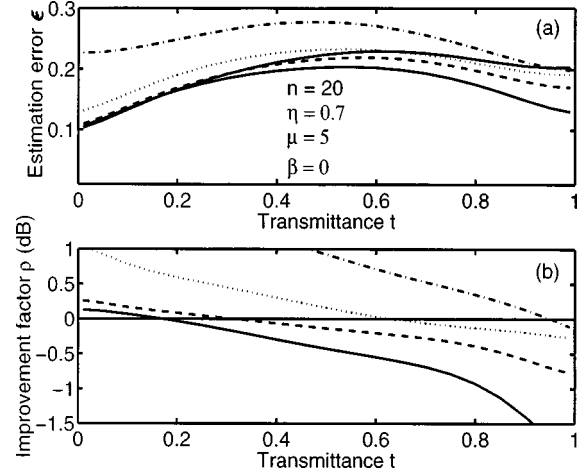


Fig. 5. (a) Estimation error ϵ as a function of the transmittance parameter t for the various estimators: Poissonian single-beam ML estimator $\hat{t}_{P,ML}$ (top solid curve), fixed-photon-number ML estimator $\hat{t}_{F,ML}$ (bottom solid curve), photon-correlated-beams ML estimator $\hat{t}_{C,ML}$ (dashed curve), count-ratio estimator $\hat{t}_{C,R}$ (dotted curve), and count-difference estimator $\hat{t}_{C,D}$ (dotted-dashed curve). The estimation parameters are $n = 20$, $\eta_s = \eta_i = 0.7$, $\mu_s = \mu_i = 5$, and $\beta = 0$. (b) Improvement factor ρ as a function of t .

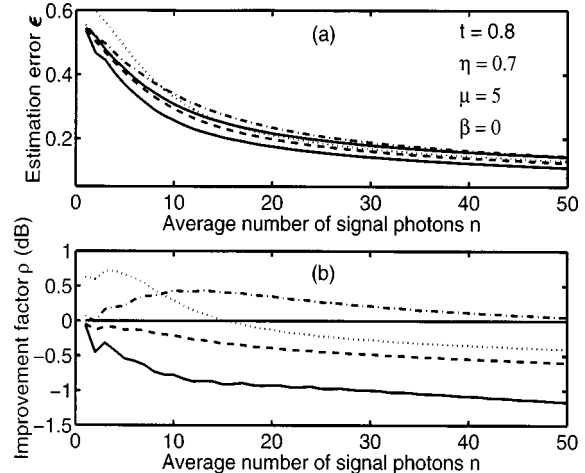


Fig. 6. (a) Estimation error ϵ as a function of the mean number of signal photons n for the various estimators: Poissonian single-beam ML estimator $\hat{t}_{P,ML}$ (top solid curve), fixed-photon-number ML estimator $\hat{t}_{F,ML}$ (bottom solid curve), photon-correlated-beams ML estimator $\hat{t}_{C,ML}$ (dashed curve), count-ratio estimator $\hat{t}_{C,R}$ (dotted curve), and count-difference estimator $\hat{t}_{C,D}$ (dotted-dashed curve). The estimation parameters are $T = 1$, $t = 0.8$, $\eta_s = \eta_i = 0.7$, $\mu_s = \mu_i = 5$, and $\beta = 0$. (b) Improvement factor ρ as a function of n .

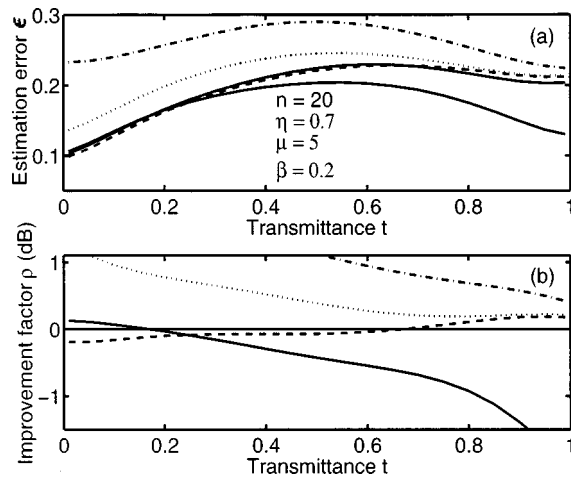


Fig. 7. (a) Estimation error ϵ as a function of the transmittance parameter t for the various estimators: Poissonian single-beam ML estimator $\hat{t}_{P,ML}$ (top solid curve), fixed-photon-number ML estimator $\hat{t}_{F,ML}$ (bottom solid curve), photon-correlated-beams ML estimator $\hat{t}_{C,ML}$ (dashed curve), count-ratio estimator $\hat{t}_{C,R}$ (dotted curve), and count-difference estimator $\hat{t}_{C,D}$ (dotted-dashed curve). The estimation parameters are $T = 1$, $n = 20$, $\eta_s = \eta_i = 0.7$, $\mu_s = \mu_i = 5$, and $\beta = 0.2$. (b) Improvement factor ρ as a function of t .

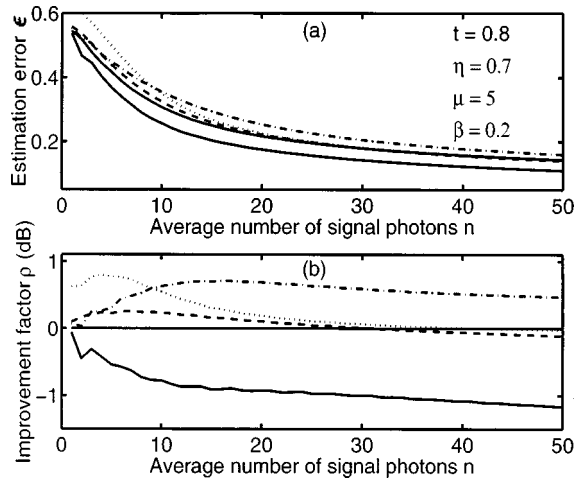


Fig. 8. (a) Estimation error ϵ as a function of the mean number of signal photons n for the various estimators: Poissonian single-beam ML estimator $\hat{t}_{P,ML}$ (top solid curve), fixed-photon-number ML estimator $\hat{t}_{F,ML}$ (bottom solid curve), photon-correlated-beams ML estimator $\hat{t}_{C,ML}$ (dashed curve), count-ratio estimator $\hat{t}_{C,R}$ (dotted curve), and count-difference estimator $\hat{t}_{C,D}$ (dotted-dashed curve). The estimation parameters are $T = 1$, $t = 0.8$, $\eta_s = \eta_i = 0.7$, $\mu_s = \mu_i = 5$, and $\beta = 0.2$. (b) Improvement factor ρ as a function of n .

D. Effect of Partial Correlation of Photons of the Twin Beams

The effect of reduced correlation ($\beta > 0$) between the photon numbers in the signal and idler beams is depicted in Figs. 7 and 8. The performance of each of the photon-correlated-beams estimators is degraded when the value of β is changed from 0 to 0.2. For $n = 20$ and for the set of parameters $\eta_s = \eta_i = 0.7$, $\mu_s = \mu_i = 5$, and $\beta = 0.2$, the photon-correlated-beams ML estimator $\hat{t}_{C,ML}$ remains superior to the Poissonian single-beam estimator for val-

ues of the transmittance parameter $t < 0.7$. The count-ratio estimator exhibits a superior performance to that of the Poissonian single-beam estimator at higher values of n (in excess of 25), as seen in Fig. 8. Hence both of the photon-correlated-beams estimators $\hat{t}_{C,R}$ and $\hat{t}_{C,ML}$ do exhibit a performance advantage over the Poissonian single-beam estimator as long as the signal level n is beyond a certain threshold depending on the parameter β , the background-noise level, and the quantum efficiencies of the detectors.

5. CONCLUSIONS

The precision of optical measurement using classical light, under weak illumination conditions, is limited by the quantum noise and the randomness associated with the very process of photon absorption. The effect of quantum noise can be reduced by using nonclassical light (sub-Poissonian light) or by using a pair of beams exhibiting positively correlated photon counts. This paper establishes the theory for developing and analyzing estimators of the optical transmittance by using a pair of photon-correlated beams generated by parametric down-conversion. We have developed three estimators of the transmittance based on the photon counts from the photon-correlated beams: the maximum-likelihood (ML) estimator, the count-ratio estimator, and the count-difference estimator. The average error, which is defined as the square root of the mean square error, of each of these estimators was compared with the error associated with the Poissonian single-beam ML estimator. As a benchmark for the maximum possible improvement in the estimation performance, the estimators were compared with the ML estimator using maximally photon-number squeezed light (light with a deterministic number of photons in a fixed time interval), where the estimation error is due only to random deletion of photons.

We have shown that a reduction in the estimation error is possible in comparison with the error associated with the Poissonian single-beam estimator. This improvement in the performance depends on key factors such as the intensity of light, the level of photon correlation, the quantum efficiency of the detectors, the level of background noise, and the actual value of the transmittance. The performance of the count-ratio estimator is generally similar to that of the ML estimator except when the average photon counts are extremely low (e.g., $n < 5$ for the case when the transmittance t is 0.5). In this low-photon-count regime, the ML estimator is superior to all estimators, and the performance of the count-difference estimator is comparable with that of the two other photon-correlated beams estimators. In fact, the errors associated with the photon-correlated ML estimator and the count-ratio estimator approach the ideal-source single-beam limit as the photon count increases. For example, under ideal detection conditions and no background noise, this limit is nearly achieved when the signal photon count is in excess of 20 (assuming that $t = 0.5$). In contrast, the performance of the count-difference estimator becomes equivalent to the performance of the Poissonian single-beam estimator when the

photon count is high. Therefore, inasmuch as the count-difference estimator exhibits an improvement in the performance for transmittance values in excess of 0.5, it falls short of the Poissonian single-beam estimator for transmittance values that are less than 0.5. Hence the count-difference estimator is not always useful in exploiting the

It is convenient to define the random variable M as the sum of the detected background-noise photons N_{ni} and the detected uncorrelated signal photons N_{ui} . Consequently, M is itself Poissonian with mean $\eta_i(1 - \beta)\lambda T + \eta_i\mu_i T$. Using the law of total probability and the independence of N_t and M , we obtain

$$\begin{aligned} \mathbb{E}(N_t|N_{ii} = \ell) &= \sum_{n=0}^{\infty} n \sum_{i=0}^{\ell} \frac{\mathbb{P}(N_t = n, N_{ii} = \ell, M = i)}{\mathbb{P}(N_{ii} = \ell)} \\ &= \sum_{n=0}^{\infty} n \sum_{i=0}^{\ell} \frac{\mathbb{P}(N_{ii} = \ell|N_t = n, M = i)\mathbb{P}(N_t = n)\mathbb{P}(M = i)}{\mathbb{P}(N_{ii} = \ell)}. \end{aligned}$$

photon correlation to reduce quantum noise. Finally, by using asymptotic analysis, we have shown that a performance advantage of the count-ratio estimator over the Poissonian single-beam estimator is always possible (under the condition that the quantum efficiency of the idler-channel detector is greater than 0.5) by means of increasing the signal photon counts.

APPENDIX A: DERIVATION OF THE COUNT-RATIO ESTIMATOR

We first start with evaluating the expectation $\mathbb{E}[(N_{ss}/N_{ii})u(N_{ii})]$. By conditioning on N_{ii} , we obtain the conditional mean

$$\mathbb{E}\left[\frac{N_{ss}}{N_{ii}} u(N_{ii})|N_{ii}\right] = N_{ii}^{-1}u(N_{ii})\mathbb{E}(N_{ss}|N_{ii}).$$

Now the last expectation can be computed by first conditioning on N_t , the actual number of twin photons, and then averaging over N_t :

$$\mathbb{E}(N_{ss}|N_{ii}) = \mathbb{E}[\mathbb{E}(N_{ss}|N_{ii}, N_t)|N_{ii}].$$

Now since the correlation between N_{ss} and N_{ii} is through N_t alone, we obtain

$$\mathbb{E}(N_{ss}|N_{ii}, N_t) = \mathbb{E}(N_{ss}|N_t),$$

and the last conditional mean can be easily evaluated as

$$\mathbb{E}(N_{ss}|N_t) = t\eta_s N_t + \eta_s(\mu_s + t\beta\lambda)T.$$

Hence

$$\begin{aligned} \mathbb{E}(N_{ss}|N_{ii}) &= \mathbb{E}[\mathbb{E}(N_{ss}|N_t)|N_{ii}] \\ &= \eta_s(\mu_s + t\beta\lambda)T + t\eta_s\mathbb{E}(N_t|N_{ii}), \end{aligned}$$

from which we obtain

$$\begin{aligned} \mathbb{E}\left[\frac{N_{ss}}{N_{ii}} u(N_{ii})\right] &= \eta_s(\mu_s + t\beta\lambda)T\mathbb{E}[N_{ii}^{-1}u(N_{ii})] \\ &\quad + t\eta_s\mathbb{E}[N_{ii}^{-1}u(N_{ii})\mathbb{E}(N_t|N_{ii})]. \quad (\text{A1}) \end{aligned}$$

The key step now is to evaluate the conditional expectation $\mathbb{E}(N_t|N_{ii})$. From the definition of the conditional mean and Bayes's rule, we obtain

$$\mathbb{E}(N_t|N_{ii} = \ell) = \sum_{n=0}^{\infty} n \frac{\mathbb{P}(N_t = n, N_{ii} = \ell)}{\mathbb{P}(N_{ii} = \ell)}.$$

Observe that, conditional on $M = i$, N_{ii} is simply N_t less a randomly deleted fraction of it (with deletion probability $1 - \eta_i$). Thus

$$\begin{aligned} \mathbb{P}(N_{ii} = \ell|N_t = n, M = i) \\ = u(n - \ell + i) \binom{n}{-\ell + i} \eta_i^{\ell - i} (1 - \eta_i)^{n - \ell + i}. \end{aligned}$$

We now use the fact that

$$\begin{aligned} \mathbb{P}(N_t = n) &= (\beta\lambda)^n \exp(-\beta\lambda)/n!, \\ \mathbb{P}(M = i) &= \{\eta_i T[(1 - \beta)\lambda + \mu_i]\}^i \\ &\quad \times \exp\{-\eta_i T[(1 - \beta)\lambda + \mu_i]\}/i! \end{aligned}$$

and carry out the algebra to finally obtain

$$\mathbb{E}(N_t|N_{ii} = \ell) = (1 - \beta)\lambda \left[(1 - \eta_i)T + \frac{\ell}{\lambda + \mu_i} \right].$$

Using this last result in Eq. (A1), we obtain

$$\mathbb{E}\left[\frac{N_{ss}}{N_{ii}} u(N_{ii})\right] = \alpha_R t + \beta_R,$$

where α_R and β_R are given in Eqs. (20) and (21), respectively.

Send all correspondence to Majeed M. Hayat, Electro-Optics Program, University of Dayton, MS 0245, 300 College Park, Dayton, Ohio 45469; phone, 937-229-4521; e-mail, mhayat@engr.udayton.edu. Adel Joobeur may be reached by phone, 203-761-4294; e-mail, joobeur@sug.com. Bahaa E. A. Saleh may be reached by phone, 617-353-7176; e-mail, besaleh@enga.bu.edu.

REFERENCES

1. B. E. A. Saleh, *Photoelectron Statistics* (Springer, Berlin, 1978).
2. M. Rabbani, "Bayesian filtering of Poisson noise using local statistics," *IEEE Trans. Acoust., Speech, Signal Process.* **36**, 933-937 (1988).
3. R. E. Sequeira, J. A. Gubner, and B. E. A. Saleh, "Quantum-limited image detection," *IEEE Trans. Image Process.* **2**, 18-26 (1993).
4. B. E. A. Saleh, "Quantum noise in optical processing," in *Real-Time Optical Processing*, B. Javidi and J. Horner, eds. (Academic, New York, 1994), pp. 407-437.
5. L. Mandel and E. Wolf, *Optical Coherence and Quantum*

- Optics* (Cambridge U. Press, Cambridge, UK, 1995). Sect. 22.4.
6. M. C. Teich and B. E. A. Saleh, "Photon bunching and antibunching," in *Progress in Optics*, E. Wolf, ed. (North-Holland, Amsterdam, 1988), pp. 1–104.
 7. B. E. A. Saleh and M. C. Teich, "Information transmission with photon-number-squeezed light," *Proc. IEEE* **80**, 451–460 (1992).
 8. S.-H. Youn, J.-H. Lee, and J.-S. Chang, "Quantum-mechanical noise characteristics in doubly resonant optical parametric oscillator," *J. Opt. Soc. Am. B* **11**, 2282–2286 (1994).
 9. B. R. Mollow, "Photon correlations in the parametric frequency splitting of light," *Phys. Rev. A* **8**, 2684–2694 (1973).
 10. C. K. Hong and L. Mandel, "Theory of parametric frequency down conversion of light," *Phys. Rev. A* **31**, 2409–2418 (1985).
 11. N. Klyshko, *Photons and Nonlinear Optics* (Gordon & Breach, New York, 1988).
 12. A. J. Joobeur, B. E. A. Saleh, and M. C. Teich, "Spatiotemporal coherence properties of entangled light beams generated by parametric down-conversion," *Phys. Rev. A* **50**, 3349–3361 (1994).
 13. A. J. Joobeur, B. E. A. Saleh, T. S. Larchuk, and M. C. Teich, "Coherence properties of entangled light beams generated by parametric down-conversion: theory and experiment," *Phys. Rev. A* **53**, 4360–4371 (1996).
 14. P. R. Tapster, J. G. Rarity, and J. S. Satchell, "Use of parametric down-conversion to generate sub-Poisson light," *Phys. Rev. A* **37**, 2963–2967 (1988).
 15. J. G. Rarity, P. R. Tapster, and E. Jakeman, "Observation of sub-Poisson light in parametric downconversion," *Opt. Commun.* **62**, 201–206 (1987).
 16. J. G. Rarity, P. R. Tapster, J. A. Levenson, J. C. Farreau, I. Abram, J. Mertz, T. Debuisschert, A. Heidman, C. Fabre, and E. Giacobino, "Quantum correlated twin beams," *Appl. Phys. B: Photophys. Laser Chem.* **55**, 250–257 (1992).
 17. E. A. Perkins, R. J. Carr, and J. G. Rarity, "A twin-beam fibre laser light scattering system," *Meas. Sci. Technol.* **4**, 215–220 (1993).
 18. C. K. Hong, S. R. Friberg, and L. Mandel, "Optical communication channel based on coincident photon pairs," *Appl. Opt.* **24**, 3877–3882 (1985).
 19. L. Mandel, "Proposal for almost noise-free optical communication under conditions of high background," *J. Opt. Soc. Am. B* **1**, 108–110 (1984).
 20. E. Jakeman and J. G. Rarity, "The use of pair production processes to reduce quantum noise in transmission measurement," *Opt. Commun.* **59**, 219–223 (1986).
 21. H. V. Poor, *Introduction to Signal Detection and Estimation* (Springer-Verlag, New York, 1988).
 22. L. Mandel, "Sub-Poissonian photon statistics in resonance fluorescence," *Opt. Lett.* **4**, 205–207 (1979).
 23. H. Stark and J. W. Woods, *Probability, Random Processes, and Estimation Theory for Engineers* (Prentice-Hall, Upper Saddle River, N.J., 1994).
 24. B. E. A. Saleh, "Quantum imaging," invited paper presented at the 1997 OSA Annual Meeting, Long Beach, Calif., 1997.
 25. B. Huttner, J. J. Baumberg, and J. F. Ryan, "Detection of short pulses of non-classical light," *Opt. Commun.* **90**, 128–132 (1992).
 26. J. K. Breslin and G. J. Milburn, "Conditional variance reduction by measurements on correlated field modes," *Phys. Rev. A* **55**, 1430–1436 (1997).